Correspondence between the coupling model predictions and computer simulations. Diffusion of a probe polymer in a matrix having different degrees of polymerization

ARTICLE *in* MACROMOLECULES · APRIL 1991

Impact Factor: 5.8 · DOI: 10.1021/ma00007a018

2 AUTHORS:

Kia L Ngai
Università di Pisa
554 PUBLICATIONS **18,304** CITATIONS
SEE PROFILE

Jeffrey Skolnick
Georgia Institute of Technology
391 PUBLICATIONS **17,219** CITATIONS
SEE PROFILE

Correspondence between the Coupling Model Predictions and Computer Simulations: Diffusion of a Probe Polymer in a Matrix Having Different Degrees of Polymerization

K. L. Ngai*

Naval Research Laboratory, Washington, D.C. 20375-5000

Jeffrey Skolnick

Departments of Molecular Biology and Chemistry, Scripps Clinic and Research Foundation, 10666 North Torrey Pines Road, La Jolla, California 92037

Received September 14, 1990

ABSTRACT: Detailed agreements between the predictions of the coupling model and the results of Monte Carlo simulations and a molecular dynamics simulation on the dynamics of the center-of-mass diffusion of entangled multichain systems are pointed out. These are further discussed in conjunction with real experimental data.

I. Introduction

For some time, one of us has proposed and subsequently in collaborations with others developed a scheme based on rather general physical principles and/or requirements for the description of relaxations of complex correlated systems,[1-4] one example of which is an entangled monodisperse linear polymer melt. The general applicability of this theoretical scheme to many different complex correlated systems has been amply demonstrated by comparison with experimental data.[5] When specialized to the case of an entangled polymer melt, and in particular to polymer self-diffusion or probe chain diffusion, the theory suggested that at very short times each chain relaxes independently, as if the other chains were absent. That is, the relaxation process is well described by simple Rouse dynamics. This Rouse-like behavior persists until a certain characteristic time, ω_c^{-1} (the magnitude of which is a characteristic of the mutual interactions between chains), when the effects due to the cooperative dynamics with other chains become apparent. Thus, the initial Rouse relaxation rate, W_0, of a chain is diminished. In the time regime when $\omega_c t > 1$, the relaxation rate of a chain is suggested to exhibit the self-similar time dependence

$$W(t) = W_0(\omega_c t)^{-n} \tag{1}$$

where $0 < n < 1$ is the coupling parameter. The normalized correlation function $Q(t)$ for the relaxation of a particular mode of a chain can be determined by solving

$$dQ/dt = -W_0(\omega_c t)^{-n}Q \tag{2}$$

which has the solution

$$Q(t) = \exp[-(t/\tau)^{1-n}] \tag{3}$$

Here, τ is related to the Rouse relaxation time τ_0 ($\equiv 1/W_0$) by the very important and useful "second" relation

$$\tau = \{(1-n)\omega_c^{\,n}\tau_0\}^{1/1-n} \tag{4}$$

Unfortunately, the theory lacks the ability to calculate n. To apply the theory, n has to be determined by comparing one of the theoretical predictions with an experimental measurement.[6,7] After n is extracted, other predictions from eq 4 can be stringently tested by comparison with additional experimental data. Representative examples of this type of analysis are polymeric self-diffusion constants[7] and terminal shear relaxation.[6]

Dynamic Monte Carlo (MC) simulations have been established as another fruitful approach to describe the dynamics of entangled polymers. In previous MC studies by Kolinski, Skolnick, and Yaris[8] (KSY), the model consists of a collection of monodisperse or bidisperse chains confined to a lattice. Each polymer chain occupies N_l lattice sites, there are N polymers per MC box, and ϕ is the volume fraction of occupied sites. The initial configuration is carefully equilibrated to ensure that the equilibrium properties are correct before proceeding to an analysis of the dynamics. An appropriate set of elementary motions is chosen to reproduce the dynamics of real lattice chains with excluded volume. Random elementary local motions of every polymer bead in all of the chains are attempted. The time unit is defined as when every polymer bead experiences on average all of the local elemental moves. Then the computer experiment is run to long times, and the dynamics of the entangled polymer chains can be deduced from the data.

A different approach to computer simulation of entangled polymers has been attempted by Pakula and coworkers[9] in a completely dense system on a lattice. In this case, the only way to move a portion of a chain is by a series of simultaneous cooperative moves involving pieces of several chains.

Alternatively, the dynamics can be simulated by Newton's equations of motion for a system that is coupled to a heat bath. Using this approach Kremer and Grest[10] have undertaken a series of homopolymeric polymer melt simulations. As shown below, their results for the center-of-mass motion are in qualitative and even semiquantitative agreement with the MC dynamics simulation of a polymer melt by KSY and by Pakula et al.

In the present paper, the principal aim is to compare the MC simulations and recent molecular dynamics simulations with the coupling scheme and to demonstrate that the results of the computer experiments provide support for the coupling model as applied to polymer dynamics.

* To whom correspondence should be addressed.

0024-9297/91/2224-1561$02.50/0

II. Relation of the Coupling Theory to Monte Carlo Simulations

Results of simulations of the dynamics of multichain systems confined to different lattices indicate that the dynamics of chains are Rouse-like at short times. One piece of evidence comes from the center-of-mass autocorrelation function, $g_{cm}(t)$, defined as

$$g_{cm}(t) = \langle [\mathbf{R}_{cm}(t) - \mathbf{R}_{cm}(0)]^2 \rangle \tag{5}$$

with $\mathbf{R}_{cm}(t)$ the vector locating the center of mass at time t. $g_{cm}(t)$ is obtained as an average over the trajectories of all of the chains in the model system. At a very short time, $g_{cm}(t)$ has the Rouse-like time dependence given by

$$g_{cm}(t) \sim t \tag{6}$$

which are therefore in accord with the center-of-mass motion of Rouse-like chains. Thus, there is an initial time regime that even in dense systems the dynamics of chains are Rouse-like. At some time scale, t_c, corresponding to displacement distances of $g_{cm}(t)$ of the order of a single chain segment, well-defined deviations from Rouse-like results begin. The onset at a finite time, t_c, of the deviation with Rouse dynamics of a chain is in agreement with the coupling scheme where the quantity ω_c^{-1} can now be identified with t_c of the MC simulation.

Next we shall show that the deviations from Rouse dynamics for $t > t_c$ (or $\omega_c t > 1$) can be related to a slowing down of relaxation rate, given by eq 1.

Actually, the single-bead autocorrelation function defined by

$$g(t) = \frac{1}{N}\sum_{i=1}^{N} |\mathbf{r}_i(t) - \mathbf{r}_i(0)|^2 = \frac{1}{N}\sum_{i=1}^{N} g_i(t) \tag{7}$$

obtained from the MC simulations has been shown by KSY[8] to correspond to slowed-down, Rouse-like motions. There the fits to the beaded profiles require that an apparent time-dependent self-diffusion coefficient of the center of mass obtained from $D(t) = g_{cm}(t)/6t$ must be used. The approach here is different, and we shall focus on $g_{cm}(t)$ instead of $g_i(t)$ or the average over all beads $g(t)$. The deviation of $g_{cm}(t)$ from Rouse behavior given by eq 6 appears as a crossover at $t > t_c$ (corresponding to distances such that $l^2 < g_{cm}(t) < 2\langle S^2 \rangle$, where $\langle S^2 \rangle$ is the mean-square radius of gyration and l the bond length) to a simple scaling relation

$$g_{cm}(t) \sim t^a, \quad a < 1 \tag{8}$$

The scaling relation (8) is exact in the range of statistical accuracy, and there are no systematic deviations, except very close to the vicinity of $2\langle S^2 \rangle$, where the t^a regime crosses over into the long-time diffusion limit; namely

$$g_{cm}(t) = 6D^*t + \text{constant} \tag{9}$$

where the constant has a small positive value and reflects the faster motion over the initial t^a regime. As chain length increases, the exponent a decreases, presumably reflecting more and more constrained motion. Here, and in what follows, we use D^* to refer to diffusion constants extracted from simulations.

MC simulations of dense cubic lattice multichain systems found[8] that a decreases from the value of 0.909 at $N = 64$, to 0.890 at $N = 100$, to 0.839 at $N = 216$, and to $N = 0.705$ at the longest $N = 800$ studied. It was also shown that in this range of chain lengths N there is a crossover from a weaker dependence of the diffusion coefficient, $D^* \sim N^{-1}$, on chain length for Rouse chains

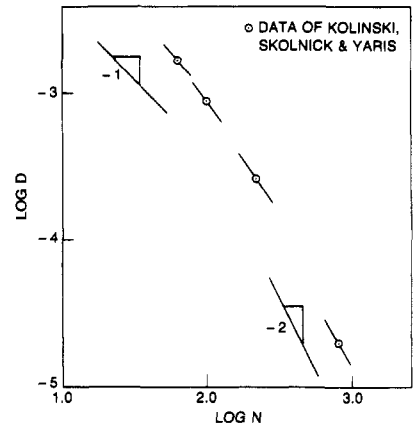

Figure 1. A log–log plot of D^*, the center-of-mass diffusion coefficient, vs N, the number of beads. The data in open circles are from Kolinski, Skolnick, and Yaris.[8] The solid straight lines drawn through each data point represent the approximate local slopes of the variation of log D^* with log N predicted by the coupling model and given by eq 44.

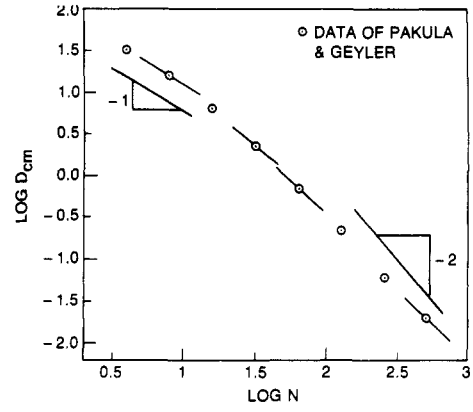

Figure 2. Same as for Figure 1 except the data are from the computer simulation of Pakula and Geyler.[9]

to a much stronger one consistent with a

$$D^* \sim N^{-2} \tag{10}$$

dependence (Figure 1).

We point out that a similar t^a behavior of $g_{cm}(t)$ has been observed by all MC simulations, including an off-lattice one by Bishop et al.,[11] an earlier study by Kremer,[12] a study of lattice systems with completely filled space by Pakula and co-workers,[9] and even in a molecular dynamics simulation of Kremer and Grest.[10] In the last two studies, both the decrease of the exponent a and the crossover of the N dependence of D^* from N^{-1} to N^{-2} with increasing chain length were obtained (see Figures 2 and 3). The values of a are comparable and even its minimal value of about 0.7 attained at the longest chain length studied in each simulation is about the same for all simulations. This deviation from Rouse behavior as given in eq 8 cannot be explained by the reptation model of polymer melt dynamics.[13] From reptation, one expects (see eq 3.10b of ref 10)

$$g_{cm}(t) \sim t^{1/2} \tag{11}$$

in the intermediate time regime of $t < \tau_{Rouse}$, where $\tau_{Rouse} = \zeta N\langle S^2(N)\rangle/3\pi^2 kT$, and

$$g_{cm}(t) \sim t \tag{12}$$

for $t > \tau_{Rouse}$. Thus, the time behavior of the center-of-mass motion predicted from the reptation model is in disagreement with all three major computer simulations. However, we shall show that this anomalous t^a time

dependence eq 8 for $l^2 \leq g_{cm}(t) \leq 2\langle S^2\rangle$ and the resumption at long times of the diffusion limit of eq 9 can be derived from the coupling scheme. As shown by Orwoll and Stockmayer,[14] a freely jointed chain of $N + 1$ beads has the translational diffusion coefficient D_0 given in terms of the longest Rouse relaxation time τ_1 by

$$D_0 = Nb^2/(3\pi^2\tau_1) \tag{13}$$

A reasonable choice for the mean-square displacement of the center of mass that corresponds to global chain diffusion is $\langle S^2\rangle$, the mean-square radius of gyration. From the relation

$$\langle S^2\rangle = (1/6)Nb^2 \tag{14}$$

we rewrite eq 13 as

$$D_0 = \langle S^2\rangle\lambda_0/3 \tag{15}$$

where

$$\lambda_0 = \frac{6}{\pi^2\tau_1} \tag{16}$$

can be considered as the diffusion rate.

If $P(\mathbf{R},t)$ is the probability of the center of mass being at $\mathbf{R}$ at time t, it is a solution to the diffusion equation

$$\frac{\partial P(\mathbf{R},t)}{\partial t} = (\langle S\rangle^2/6)(2\lambda_0)\nabla^2 P(\mathbf{R},t) \tag{17}$$

There is an alternative way of arriving at the previous equation by considering the center-of-mass diffusion as a continuous-time random walk (CTRW) process with step length or walk distance of

$$c_0 = \langle S^2\rangle^{1/2} \tag{18}$$

and a transition time distribution function

$$\psi(t) = \lambda_0 \exp(-\lambda_0 t) \tag{19}$$

The exponential nature of the transition time distribution function reflects a classical Markov process corresponding to diffusion with a time-independent diffusion rate λ_0 as represented by eq 17. The mathematical framework of the CTRW process is well documented by Montroll and Weiss.[15] Its use in the formulation of dispersive translational diffusion was made earlier by Ngai and Liu.[16] These results (see sections II and IIB and Appendix C of ref 16) will be taken over in the present considerations. Center-of-mass diffusion is now described by the equation

$$\frac{\partial P(\mathbf{R},t)}{\partial t} = (c_0^2/6)\int_0^t \phi(t-t')\nabla^2 P(\mathbf{R},t')\,dt' \tag{20}$$

where $\phi(t)$ is the memory function. In the CTRW formalism the Laplace transform $\phi^*(u)$ of $\phi(t)$ is related to the Laplace transform $\psi^*(u)$ of $\psi(t)$ by

$$\phi^*(u) = u\psi^*(u)/[1 - \psi^*(u)] \tag{21}$$

It can be verified that for $\psi(t)$ given by eq 19

$$\phi(t) = 2\lambda_0\delta(t) \tag{22}$$

where $\delta(t)$ is the delta function. Upon substitution of this expression for $\phi(t)$ into eq 20, we recover the original diffusion equation (17).

In the CTRW formulation, the random walk is described by the probability $Q(t)$ that the center of mass, initially at a site, will remain at the same site at a later time. For random walks of distance c_0 with a time-independent transition rate of λ_0, $Q(t)$ satisfies the rate equation

$$dQ/dt = -\lambda_0 Q \tag{23}$$

The transition time distribution function $\psi(t)$ is defined by

$$\psi(t) = -dQ/dt \tag{24}$$

It is now clear that the expression for $\psi(t)$ given earlier in eq 19 for classical diffusion such as in Rouse chains follows from eqs 23 and 24.

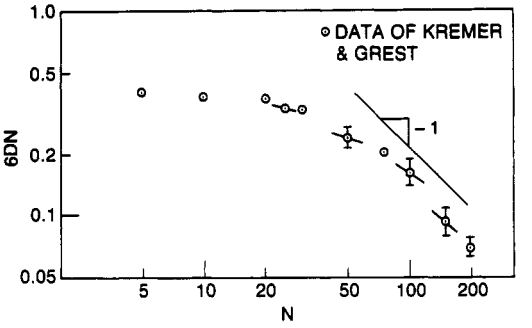

Figure 3. A log–log plot of the product $6DN$ vs N from the molecular dynamics simulation of Kremer and Grest.[10] The short solid lines drawn through some data points represent the predicted approximate local slopes of the variation of log $(6DN)$ vs log N predicted by the coupling model and given by the expression $2 - 2/a(N)$, where $a(N)$ is the exponent in the intermediate time dependence $t^{a(N)}$ of $g_{cm}(t)$.

The above discussions on the CTRW formulation of Rouse chain diffusion provide the framework for incorporating the modifications as proposed in the coupling scheme, i.e., the slowing down of the Rouse chain diffusion rate λ_0 by constraint dynamics caused by entanglements with other chains. In the coupling scheme (see eqs 1–4) the constant diffusion rate λ_0 will be slowed down to the self-similar, time-dependent form of

$$W_D(t) = \lambda_0(\omega_c t)^{-n_D} \tag{25}$$

The coupling parameter n_D for self-diffusion may not have the same value as the coupling parameter n_1 for shear deformation of the Rouse mode with the longest relaxation time because the molecular motions involved in the two processes are not the same.[7] The function $Q(t)$ now satisfies the modified rate equation

$$dQ/dt = -\lambda_0(\omega_c t)^{-n_D}Q \tag{26}$$

and it follows from eq 24 that

$$\psi(t) \equiv -dQ/dt = \lambda_0(\omega_c t)^{-n_D}\exp[-(t/\tau_D^*)^{1-n_D}] \tag{27}$$

where

$$\tau_D^* = \{(1 - n_D)\omega_c^{n_D}\lambda_0^{-1}\}^{1/(1-n_D)} \tag{28}$$

With $\psi(t)$ determined by eq 27, the mean-square displacement of the center of mass $g_{cm}(t)$ can be obtained by solving the CTRW equation (20) with the memory function $\phi(t)$ given by the inverse Laplace transform of eq 21 where $\psi^*(u)$ is the Laplace transform of $\psi(t)$, now having the slowed-down form of eq 27. The mathematical techniques for solving these equations and the solution $g_{cm}(t)$ (which is $\langle r^2(t)\rangle$ in ref 14) can be found in an earlier publication.[16] The results for $g_{cm}(t)$ were given for two time regimes, $t \ll \tau_D^*$ and $t \gg \tau_D^*$, by eqs 22, 39, C9, and 43 of ref 16. We rewrite these results here as

$$g_{cm}(t)/c_0^2 = [(1-n_D)\Gamma(1-n_D)/\{\Gamma(2-n_D)(\tau_D^*)^{1-n_D}\}]t^{1-n_D} \quad \text{if } t \ll \tau_D^* \quad (29a)$$

$$= [1/\Gamma(1+1/(1-n_D))](t/\tau_D^*) \quad \text{if } t \gg \tau_D^* \quad (29b)$$

It can be seen immediately from the equations above that the $g_{cm}(t)$ predicted by the coupling scheme has a t^a dependence as given by eq 8 within the intermediate time regime with

$$a = 1 - n_D \quad (29c)$$

and the diffusive t dependence as given by eq 9 in the long time regime. Both features have been obtained by computer simulations.[8-10] The questions remain as to the magnitude of n_D and its dependence on N.

For $N \ll N_e$, the polymer chains do not entangle. The absence of entanglement coupling requires n_D to vanish. As N is increased to approach N_e, the dynamical constraints between chains are enhanced, and n_D increases monotonically. When $N \gg N_e$, that is, well into the entanglement regime, n_D will plateau to a constant value. This is because the number of entanglements will then increase proportionally with N/N_e, a self-similar situation, and the coupling parameter will remain constant. We can calculate this plateau value of n_D by comparing the predictions on the N (or molecular weight M) and temperature dependencies of $g_{cm}(t)$ with either computer experiment or real self-diffusion experimental data[5,7] of fully entangled systems. The self-diffusion constant D^* is obtained by comparing eq 29b with eq 9 for large t as

$$D^* = (\langle S^2\rangle/6\tau_D^*)[(1-n_D)/\Gamma(2-n_D)] \quad (30)$$

where

$$\tau_D^* = \{(\pi^2/6)(1-n_D)\omega_c^{n_D}\tau_1\}^{1/(1-n_D)} \quad (31)$$

The pair of equations (32) and (33) have been obtained before[5,7] by a different approach based on an argument due to de Gennes[13] that

$$D^* \sim \langle S^2\rangle/\tau_D^* \quad (32)$$

Equations 30, 28, and 16 can be used to derive the N and T dependencies of D^*. We use the expression for the first Rouse mode relaxation times τ_1

$$\tau_1 = N^2\langle l^2\rangle_0\zeta_0/(3\pi^2 k_B T) \quad (33)$$

where ζ_0 is the temperature-dependent monomer friction coefficient and $\langle l^2\rangle$ is the effective square of the bond length. The N and T dependencies of D^* are predicted to be given by

$$D^* \sim N^{1-2/(1-n_D)} \exp\left(\frac{-E_a}{(1-n_D)k_B T}\right) \quad (34)$$

We have assumed here the special case that the Rouse monomeric friction coefficient ζ_0 has an Arrhenius temperature dependence

$$\zeta_0 \propto \exp(E_a/k_B T) \quad (35)$$

where E_a may be identified with the internal rotation isomerism energy barrier, as is appropriate for polymers with low glass temperature such as polyethylene and hydrogenated polybutadiene.[5,7]

By equating the molecular weight exponent in eq 34 to the value of approximately −2 obtained in computer simulations and actual experiments, i.e.

$$1 - 2/(1-n_D) = 2 \quad (36)$$

the value

$$n_D = 0.33 \quad (37)$$

is extracted.[5,7] Alternatively, as done in ref 7, by equating the measured activation energy E_a^* of the self-diffusion coefficient of polyethylene or hydrogenated polybutadiene to the prediction of eq 34

$$E_a^* = E_a/(1-n_D) \quad (38)$$

and knowing E_a from other sources,[6,7] the value

$$n_D = 0.32 \quad (39)$$

had been deduced. As discussed in the Introduction, although the coupling scheme does not provide a calculation of n_D, the multiple predictions it makes as exemplified by eq 34 offer a number of ways to extract its value from experiment. We can use one prediction, say eq 38, to determine n_D from experimental data. After the value 0.32 of n_D is determined this way from eq 38, we use it to predict for $N \gg N_e$ that

$$\text{(i) } D^* \sim N^{-1.94} \quad (40)$$

for the molecular weight dependence of D^* from eq 34 and that

$$\text{(ii) } g_{cm}(t) \sim t^{0.68}, \quad \text{for } t < \tau_D^* \quad (41)$$

from eq 29a for fully entangled systems. Prediction i is in good agreement with the well-known N^{-2} dependence of self-diffusion experimentally observed in many, though not all, polymers. Prediction ii holds for the regime of $N \gg N_e$ only. Computer simulations are invariably limited by available computation time, and in all published simulations, the simulations are terminated at sufficiently large N to ensure crossover from the Rouse regime with $D \sim N^{-1}$ to the $D \sim N^{-2}$ regime. The minimal values of the exponent of eq 8 obtained for the largest N by Kolinski et al.[8] and Kremer and Grest[10] are respectively 0.69 and 0.70. These values are in good agreement with the predicted exponent of 0.68 given in eq 41.

In all computer simulations,[8-10] it is found that, as N increases to crossover from the Rouse regime to the entangled regime, the exponent a decreases monotonically from 1.0 toward the minimal plateau value of about 0.68, while the exponent α of $D^* \sim N^{-\alpha}$ increases monotonically from 1.0 to approach the plateau value of 2.0 (see Figures 1–3). The trends in the variations of the exponents a and α as well as their correlation are easy to explain. For small N such that its chain dynamics are essentially Rouse-like at all times, $n_D \cong 0$ because the chains are independent. For $N \gg N_e$, the chains are fully entangled, the chain dynamics are cooperative, and n_D appears to reach the plateau value of 0.32–0.33. In the crossover region, the coupling scheme expects[17,18] that n_D increases monotonically with N because the dynamical constraints increase also monotonically with N. Although eq 34 is strictly valid when n_D is a constant independent of N, the expression is a reasonable approximation for the exponent α

$$\alpha \cong 2/(1-n_D) - 1 \quad (42)$$

The exact procedure is to calculate D^* as a function of N from eqs 30 and 31 with n_D as a function of N taken from computer simulation data. The exponent α is then obtained as a function of N by taking the derivative $-\mathrm{d}\log D^*/\mathrm{d}\log N$. However, this procedure is impractical here because computer simulations do not give the actual physical value of ω_c. Nevertheless, we expect this exact value of α will be well approximated by the right-hand

side of eq 42 when the variation of n_D with N is not fast. By inspection of the relation for the exponents given by eqs 29c and 42, it is clear that the coupling scheme predicts that

$$\alpha = 2/a - 1 \tag{43}$$

i.e., a correlation of the decrease of a with the increase in α.

Actually, we can go further in the comparison of the predictions, eqs 29c, 31, 42, and 43 of the coupling scheme, with the three major computer simulations. From the intermediate time $t^{a(N)}$ dependencies of $g_{cm}(t)$, eqs 8 and 29a, obtained by computer simulations for an N-chain, we deduce the corresponding coupling parameter $n_D(N)$ from eq 29c. With $n_D(N)$ determined, the exponent $\alpha(N)$ can be calculated by eq 42. In this manner, the coupling model permits us to predict approximately (because eq 42 is not exact) the local slope at N of the log $D(N)$ versus log N plot of the computer simulation data; i.e.

$$\partial \log D^*(N)/\partial \log N \equiv -\alpha(N) \cong 1 - 2/a(N) \tag{44}$$

The predicted values of local slopes are indicated in Figures 1–3, where log–log plots of either $6D^*$ or $6DN$ vs N for the KSY, Pakula–Geyler, and Kremer–Grest simulations are shown. In Figures 1 and 2, the diffusion coefficients obtained from two computer simulations[8,9] are plotted separately as open circles. The short solid lines through data points are the approximate tangents to a log–log plot at points $(N,6D^*(N))$ with slopes $1 - 2/a(N)$ calculated from eq 44 of the continuous curve obtained by interpolation of the discrete computer simulation data. Similarly, in Figure 3, the short solid lines through data points are the approximate tangents at points $(N,6D^*N)$ with slopes $2 - 2/(1 - N_D)$ in a log–log plot of data from ref 10. By inspection of Figures 1–3, the coupling scheme predictions seem to be in good agreement with the computer experiments for the center-of-mass autocorrelation functions $g_{cm}(t)$ and self-diffusion coefficients D^*. Thus, not only is the form of $g_{cm}(t)$ obtained by computer simulations, eqs 8 and 9, in agreement with the coupling scheme predictions, eqs 29a and 29b, but also correlations between the exponent a and the variation of D^* with chain length N are expected by the coupling scheme for monodisperse systems. In other words, using the exponent $a(N)$ provided by the computer data, the variation of D^* with N predicted by the coupling scheme is in good agreement with the data. In particular, for large N, the coupling scheme correctly predicts the $D^* \sim N^{-2}$ (see eqs 40 and 41).

III. Dynamics of a Probe Chain in a Matrix of Different Degrees of Polymerization

Monte Carlo simulations of the dynamics of a probe chain of size N_p dissolved in a matrix of polymers, each containing N_m beads, have also been performed.[8] All the computational MC experiments were performed at a single total volume fraction of polymer $\phi = 0.5$, where $\phi_p + \phi_m$ is the sum of the contributions from probe polymers and matrix polymers, respectively. The value of ϕ_p was always much lower (by a factor of 32–40) than ϕ_m. To date, only the dynamics of a probe chain consisting of $N_p = 100$ segments in a matrix of chains of the length of $N_m = 50$ up to $N_m = 800$ have been simulated by means of cubic lattice MC calculations. As we shall see, for reasons to be discussed it is desirable to have simulations for probe chains of $N_p = 800$ and $N_m = 50$ up to 8000. Unfortunately, the computations for $N_p = 800$ and $N_m \gg N_p$ are extremely time-consuming, and they are not feasible at this time.

The mean-square displacement of the center of mass $g_{cm}(t)$ of the probe polymer with $N_p = 100$ in various linear-chain matrices up to $N_m = 800$ has time dependencies also given by eqs 8 and 9, as in the homopolymeric ($N_p = N_m$) melt case. The continuous-time random walk calculation of $g_{cm}(t)$ based on the coupling scheme given in the previous section applies also for a probe chain in a matrix. The results for $g_{cm}(t)$ can be taken from eqs 29–31. In order to distinguish the coupling parameter for a probe chain dissolved in a matrix from that for a chain in the homopolymeric melt, we use n_p and a_p instead of n_D and a, respectively. The results for $g_{cm}(t)$ of the probe chain from MC simulations[8] and from the coupling scheme, eqs 29a and 29b, are again identical. Thus, we may also conclude that probe chain dynamics are consistent with the coupling scheme description.

Although the coupling model does not provide a calculation of the coupling parameter of a probe chain in any matrix, it can rationalize the trend of the variation of n_p with N_m for fixed N_p. If N_p is sufficiently large that in the homopolymeric melt, $N_m = N_p$, the chain experiences significant entanglement coupling with other chains, then the homopolymeric coupling parameter n_D has a nonzero value. This is the case for the probe chain consisting of $N_p = 100$ segments studied by MC simulations because when $N_m = N_p = 100$, $a = 0.890$ and $n_D = 0.11$ is nonzero. The coupling parameter of the coupling model in eq 1 is a measure of the slowing down of the Rouse rate of a probe chain resulting from the coupling with other chains. Starting from the homopolymer with $N_p = N_m$, consider what happens if N_m of the matrix is reduced such that $N_m < N_p$. The matrix chains now being shorter will relax faster than the probe chain, and therefore the dynamic constraints they impose on the probe chain in the homopolymer will be reduced. In other words, part of the dynamical constraints in the $N_m = N_p$ homopolymer are mitigated in a matrix with $N_m < N_p$. Using a constraint dynamics formulation[4,17,18] of the coupling scheme, we would expect from mitigation of dynamical constraints that the coupling parameter n_p will be reduced from the homopolymer value n_D, i.e.

$$n_p < n_D, \quad \text{if } N_m < N_p \tag{45}$$

or

$$a_p > a, \quad \text{if } N_m < N_p \tag{46}$$

On the other hand, if $N_m > N_p$ the matrix chains become longer and relax slower than the probe chain. Dynamic constraints on the probe chain will be enhanced in higher N_m matrices as compared with that in the homopolymeric melt. From the coupling theory, one expects that

$$n_p > n_D, \quad \text{if } N_m > N_p \tag{47}$$

or

$$a_p < a, \quad \text{if } N_m > N_p \tag{48}$$

These predictions for the trend of n_p or a_p with N_m are verified by the results of MC simulations. In fact, a probe polymer with $N_p = 100$ has $a = 0.890$ in the homopolymer. In a matrix of shorter length $N_m = 50$, $a_p = 0.958$ is larger than a, in agreement with eq 46, while in matrices of longer lengths $N_m = 216$ and 800, $a_p = 0.883$ and 0.825, respectively. The decrease of a_p with increasing N_m is also in agreement with eq 48.

Associated with the decrease of a_p with increasing N_m, the MC simulations find that the diffusion coefficients D^* also decrease; the decrease is about 30% over the range of N_m studied. This dependence of D^* also follows as the consequence of another prediction of the coupling scheme from eqs 30 and 31 after being generalized to probe

diffusion as

$$D^* = (\langle S^2 \rangle / 6\tau_p^*)[(1 - n_p)/\Gamma(2 - n_p)] \quad (49)$$

and

$$\tau_p^* = \{(\pi^2/6)(1 - n_p)\omega_c^{n_p}\tau_1\}^{1/(1-n_p)} \quad (50)$$

Since $\omega_c\tau_1 \gg 1$, it is not difficult to see from eq 50 that τ_p^* increases with n_p. Hence from eq 49 D^*, being inversely proportional to τ_p^*, is expected to decrease with increasing n_p or decreasing a_p as found by MC simulations.

It is interesting to point out that the increases of both the coupling parameter n_p of the probe chain with N_p = 100 and the effective relaxation time τ_p^* when going from the homopolymer to a matrix with N_m = 800 from MC experiment seem to correspond to what was observed in a real experiment using infrared dichroism to measure relaxations in a bidisperse melt.[19] A binary blend consisting of nearly monodisperse hydrogenated polyisoprenes of molecular weights 53 000 and 370 000, both several times the entanglement molecular weight, was studied. From the published results we find that the short chains in a homopolymer melt with 100% short chains relax with a time dependence approximately consistent with a stretched exponential, eq 3, with n roughly between 0.3 and 0.4. An accurate determination of n is hampered by limited data of slightly over a decade in time. In blends with increasing volume percentage of long chains, the short-chain relaxation is shifted to longer times and becomes more dispersive, consistent with the short chains having a larger coupling parameter n and longer relaxation time τ^*. These features are in agreement with the change in dynamics of a probe chain with increasing matrix chain length from MC simulations and from what are predicted by the coupling scheme.

IV. Conclusions

In the present paper we have examined, in the context of the coupling model of polymer dynamics, the relationship between the exponent α describing the scaling of the diffusion constant with chain length, $D^* \sim N^{-\alpha}$, and the intermediate-time scaling exponent, a, of the mean-square displacement of the center of mass $g_{cm} \sim t^a$. To a reasonable approximation, we find that these two exponents are related by the approximate equation (43). Thus if $D^* \sim N^{-2}$, then $a = {}^2/_3$ and the intermediate time regime of $g_{cm}(t)$ is predicted to have a $t^{0.67}$ regime. Remarkably, all extant simulations[8-10] obtain values of 0.69–0.7 for the exponent a when the dependence of D^* approaches the N^{-2} dependence. Thus, consistency between computer simulations and the coupling model has been demonstrated. Furthermore, in subsequent work, we shall demonstrate that if the n values are independent of the particular Rouse mode, then it follows that $g(t)$, the mean-square displacement of a single bead, scales with time as $t^{a/2}$. The latter prediction is also in accord with extant simulations. However, it may be argued that since all the simulations are in the crossover regime to fully entangled behavior, the exponent a has not achieved its minimal value. If a assumes a value of ${}^1/_2$ (consistent with predictions of reptation theory), then it follows from eq 44 that $D^* \sim N^{-3}$. Unfortunately, the asymptotic scaling of D^* with N remains the object of some controversy, and additional computer simulations at longer chain lengths are required to establish the asymptotic value of a and its relationship to α. Nevertheless, based on extant simulation and experiments to date, it seems fair to conclude that the coupling model has proven capable of rationalizing the behavior of entangled polymer melts in a wide variety of situations and thus remains a viable alternative theory to the reptation model of polymer melt dynamics.

Acknowledgment. J.S. acknowledges the support of the Polymers Program of the National Science Foundation. K.L.N. is supported in part at NRL by ONR Contract N0001491WX24019.

References and Notes

(1) Ngai, K. L. *Comments Solid State Phys.* **1979**, *9*, 127.
(2) Rajagopal, A. K.; Ngai, K. L.; Teitler, S. *J. Phys. C: Solid State Phys.* **1984**, *17*, 6611.
(3) Ngai, K. L.; Rajagopal, A. K. In *Non-Debye Relaxation in Condensed Matter*; Ramakrishran, T. V., Lakshimim, Raj., Eds.; World Scientific: New York, 1987.
(4) Ngai, K. L.; Rajagopal, A. K.; Teitler, S. *J. Chem. Phys.* **1988**, *88*, 5086.
(5) For a review, see: Ngai, K. L.; Rendell, R. W.; Rajagopal, A. K.; Teitler, S. *Ann. N.Y. Acad. Sci.* **1986**, *484*, 150.
(6) Ngai, K. L.; Plazek, D. J. *J. Polym. Sci., Polym. Phys. Ed* **1985**, *23*, 2159.
(7) McKenna, G. B.; Ngai, K. L.; Plazek, D. J. *Polymer* **1985**, *26*, 1651.
(8) Kolinski, A.; Skolnick, J.; Yaris, R. *J. Chem. Phys.* **1987**, *84*, 1992; **1987**, *86*, 1567; **1987**, *86*, 7164; **1987**, *86*, 7174, and references therein.
(9) Pakula, T. *Macromolecules* **1987**, *20*, 679. Pakula, T.; Geyler, S. *Macromolecules* **1987**, *20*, 2909; **1988**, *21*, 1665.
(10) Kremer, K.; Grest, G. *J. Chem. Phys.* **1990**, *92*, 5057.
(11) Bishop, M.; Ceperley, D.; Frisch, H. L.; Kalos, M. H. *J. Chem. Phys.* **1982**, *76*, 1557.
(12) Kremer, K. *Macromolecules* **1983**, *16*, 1632.
(13) de Gennes, P.-G. *Scaling Concepts in Polymer Physics*; Cornell University, Press: Ithaca, NY, 1979.
(14) Orwoll, R. A.; Stockmayer, W. H. *Adv. Chem. Phys.* **1969**, *15*, 305. Yamakawa, H. *Modern Theory of Polymer Solutions*; Harper and Row: New York, 1969.
(15) Montroll, E. W.; Weiss, G. H. *J. Math. Phys.* **1965**, *6*, 167.
(16) Ngai, K. L.; Liu, F. S. *Phys. Rev.* **1981**, *B24*, 1049. A numerical solution for $g_{cm}(t)$ that is valid for all times has been obtained by: Rendell, R. W.; Ngai, K. L. *J. Non-Cryst. Solids*, in press. The good agreement with computer simulations is noteworthy.
(17) Rajagopal, A. K.; Ngai, K. L.; Teitler, S. *Nucl. Phys. B (Proc. Suppl.)* **1988**, *5A*, 98.
(18) Ngai, K. L.; Rajagopal, A. K.; Lodge, T. P. *J. Polym. Sci., Part B: Polym. Phys.* **1990**, *28*, 1367.
(19) Kornfield, J. A.; Fuller, G. G.; Pearson, D. S. *Macromolecules* **1989**, *22*, 1334.